Determination of carrier mobility in phenylamine by time-of-flight, dark-injection, and thin film transistor techniques

Cheung, C. H.; Kwok, K. C.; Tse, S. C.; So, S. K.

Published in:
Journal of Applied Physics

DOI:
10.1063/1.2909904

Published: 01/05/2008

Document Version:
Publisher's PDF, also known as Version of record

Determination of carrier mobility in phenylamine by time-of-flight, dark-injection, and thin film transistor techniques

C. H. Cheung, K. C. Kwok, S. C. Tse, and S. K. So[a)]
Department of Physics and Centre for Advanced Luminescence Materials, Hong Kong Baptist University, Kowloon Tong, Hong Kong, China

(Received 9 December 2007; accepted 6 March 2008; published online 5 May 2008)

The hole transport property of a phenylamine-based compound, 4, 4′,4″-tris(*n*-(2-naphthyl)-*n*-phenyl-amino)-triphenylamine, was independently studied by time-of-flight (TOF), dark-injection space-charged-limited-current (DI-SCLC), and thin film transistor (TFT) techniques. With UV-ozone treated gold as the injecting anode, clear DI-SCLC transient peaks were observed over a wide range of electric fields. The hole mobilities evaluated by DI-SCLC experiment were in excellent agreement with the mobilities obtained from the TOF technique. The injection contact was demonstrated to be Ohmic by an independent current-voltage (*J*-*V*) experiment. However, with the same injecting electrode, the mobility deduced from the TFT method was found to be 9.8 $\times 10^{-7}$ $cm^2/V\,s$, which was about one order of magnitude smaller than the TOF mobility ($\sim 1.2 \times 10^{-5}$ $cm^2/V\,s$). The origin of the discrepancy is discussed.
 [DOI: 10.1063/1.2909904]

I. INTRODUCTION

The invention of efficient organic light emitting diodes (OLEDs) in the 1980s set off intensive researches on organic electronic materials for manufacturing large-area and flexible organic electronic devices.[1] In addition to OLEDs, different devices, such as photovoltaic cells[2] and thin film transistors (TFTs),[3] have been realized. In all of these devices, at least one organic material is incorporated and the devices are operated by a drift current generated either by charge injection from contact electrodes or by optical excitation. Therefore, the charge injection and charge transport mechanisms in organic solids are the crucial issues governing the performance of the devices.[4,5] With deeper understanding of the nature of carrier mobility in organic materials, we can effectively optimize the device performance.

This contribution compares three carrier mobility evaluation techniques, namely, time-of-flight (TOF), dark-injection space-charged-limited-current (DI-SCLC), and TFT techniques. Their applications to 4, 4′,4″-tris(*n*-(2-naphthyl)-*n*-phenyl-amino)-triphenylamine (2TNATA) will be examined. Figure 1 shows the chemical structure and the highest occupied molecular orbital (HOMO) energy level of 2TNATA and the work function of the charge injecting anode (Au). 2TNATA can be classified as a member of phenylamine (PA) based compounds, which are very important hole transporting materials for OLEDs.[6] PA compounds have an excellent film forming ability and satisfactory stability in air. They can also exhibit trap-free hole transporting properties, which make them ideal candidates for examining the charge transporting mechanism in amorphous organic semiconductors.[7]

Among the three carrier mobility evaluation techniques, TOF stands out, perhaps, as the most universal.[8] In TOF, the organic material under evaluation is optically excited by an UV laser to create free charge carriers for drift mobility measurements. While popular, the TOF technique has a distinct disadvantage. A thick film of several microns is required in order to have a well-defined flight distance. Besides TOF, there are established electrical techniques for the evaluation of carrier mobility. Of special interest is the DI-SCLC technique.[9] In DI-SCLC, charge carriers are electrically injected by a voltage pulse into the material. As the location of the carrier injection is now well defined, the DI-SCLC technique should require a thin sample only. However, in reality, the observed transient signal is a superposition of the sample charging current (i.e., *RC* decay) and the DI transient current. A thin sample would increase the sample capacitance *C*, rendering the observation of the true transit time difficult.

Realizing the thickness limitations of both TOF and DI-SCLC, we use a TFT configuration to evaluate the carrier mobilities in thin organic films (<100 nm). Figure 2 shows a bottom contact TFT with 2TNATA as the active material. Under a negative gate bias, a thin layer of 2TNATA adjacent to the gate dielectric forms a conducting channel. It was demonstrated that a layer of an organic material as thin as 16 nm can act as an effective channel.[10] Mobilities extracted

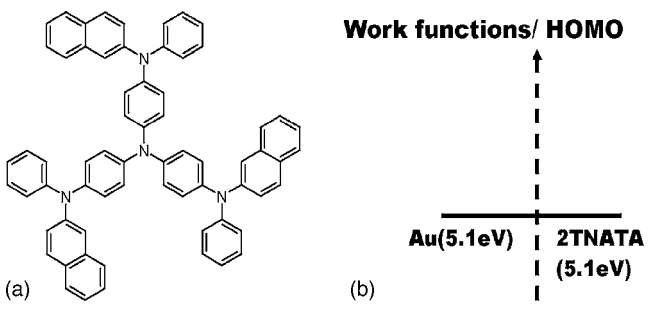

FIG. 1. (a) Chemical structure of 2TNATA; (b) HOMO level of 2TNATA and work function of the bare Au.

[a)]Author to whom correspondence should be addressed. Electronic mail: skso@hkbu.edu.hk.

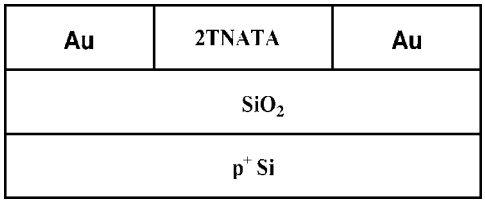

FIG. 2. A schematic of 2TNATA based OTFT with the bottom contact configuration.

from TFT are generally found to be different from TOF mobilities, but the origins are still unclear. For polycrystalline materials, some reports showed that TOF mobilities are smaller than those extracted from TFT.[11,12] On the other hand, for amorphous materials (e.g., 2TNATA), there are much fewer investigations. Below, we show that, indeed, the carrier mobilities evaluated by TOF and DI-SCLC are in good agreement with each other. However, results from TFT significantly differ from the those of the other two techniques for amorphous thin films of 2TNATA. The origins of the difference will be discussed.

II. EXPERIMENTAL

2TNATA was purchased from E-Ray and was used without further purification. The sample structure for TOF experiment was indium tin oxide (ITO)/2TNATA(7.1 μm)/Al(15 nm). Before the deposition of the 2TNATA film, ITO coated glasses were chemically cleaned by using sequential baths of deconex, de-ionized water, and acetone, which was followed by exposure to UV ozone (UVO).[13] The coating rate for 2TNATA was 1 nm/s. A semitransparent Al film was then evaporated on the organic layer. A nitrogen pulsed laser (337 nm) was incident from the Al electrode to generate free charges. Holes were attracted toward the negatively biased ITO electrode. A digital oscilloscope was used to capture the voltage across a current sensing resistor, which was connected in series to the sample. For DI-SCLC, the structure was Au(100 nm)/2TNATA(1 μm)/Au(100 nm). In order to be consistent with the TFT experiment, the bottom Au (charge injecting anode) was treated with UVO. The hole injection behavior at the Au/2TNATA contact was also examined. Since only the hole injection is examined, Au was also chosen to be the cathode as it is electron blocking. After fabrication, current-voltage (J-V) experiments were performed on the samples with a computer controlled Keithley source-measure unit (model 236). The samples were then subjected to a rectangular voltage pulse by using a pulse generator (HP model 241B). A digital oscilloscope was used to capture the current transients in a manner similar to TOF.[9] For TFT, a heavily doped p-Si wafer with an overlayer of 300 nm SiO_2 (C_i=11 nF cm^{-2}) was employed as the substrate. Gold source and drain electrodes with a channel width (W) of 9 mm and a channel length (L) of 50 μm were evaporated on the substrate. The predefined substrates were exposed to UVO. Subsequently, 2TNATA was thermally evaporated onto the substrates at a rate of 0.05 nm/s inside a high vacuum evaporator. The substrates were kept at 60 °C and the thickness of 2TNATA was 90 nm. All of the film thicknesses in our experiments were measured *in situ* by a quartz crystal sensor and *ex situ* by a step profilometer (Tencor Alpha-Step 500). After fabrication, the samples were immediately loaded inside a vacuum cryostat with a pressure of less than 10^{-3} Torr for measurements. The temperature of the samples can be regulated between 270 and 340 K.

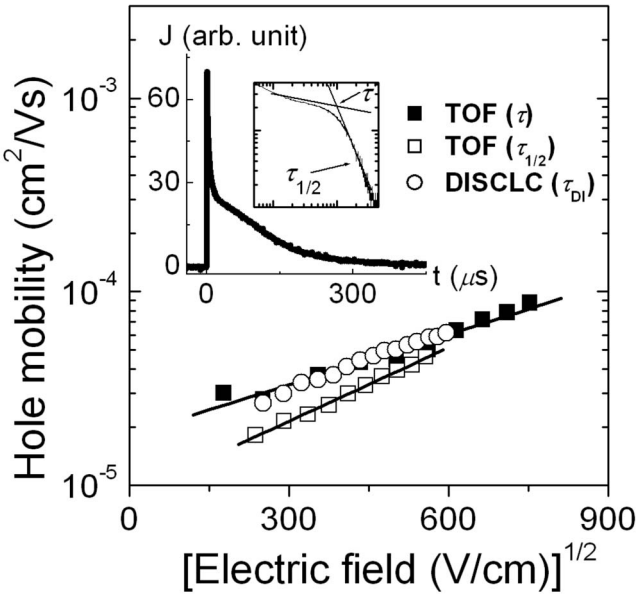

FIG. 3. The hole mobilities of 2TNATA against the square root of the electric field at 290 K derived from (a) TOF (τ) (solid squares), (b) TOF ($\tau_{1/2}$) (open squares), and (c) DI-SCLC (open circles). The inset is the TOF time transient and its log-log plot at 290 K under an applied electric field strength of 140 kV/cm.

III. RESULTS AND DISCUSSIONS

Figure 3 (inset) shows the TOF transient of 2TNATA at room temperature and at an applied field strength of F =140 kV/cm. The hole transit time can be determined from a log-log plot of the transient. In principle, the transit time τ is the arrival time of the fastest carrier in TOF. Another way to define the carrier transit time is to measure $\tau_{1/2}$, which is the time for the TOF transient signal to drop to one-half of the value in the plateau region (as shown in the inset of Fig. 3). $\tau_{1/2}$ can be regarded as the "average" carrier transit time.

The field dependent hole mobilities μ_h derived from τ (closed squares) and $\tau_{1/2}$ (open squares) are shown in Fig. 3. The hole mobilities follow the Poole–Frenkel form with $\mu_h \sim \exp(\beta F^{1/2})$. The factor β is the Poole–Frenkel slope, which can be obtained by fitting a straight line to each data set in Fig. 3. It indicates the sensitivity of the mobility in response to the applied electric field. The zero-field mobility (μ_0) can also be obtained from the straight line when F=0. The extracted β and μ_0 at room temperature for 2TNATA are shown in Table I.

TABLE I. Hole transport data of 2TNATA at room temperature (290 K) from the TOF technique.

	Extracted from τ	Extracted from $\tau_{1/2}$
Poole–Frenkel slope β [(cm/V)$^{1/2}$]	2.0×10^{-3}	2.9×10^{-3}
Zero-field mobility μ_0 (cm^2/V s)	1.8×10^{-5}	8.7×10^{-6}

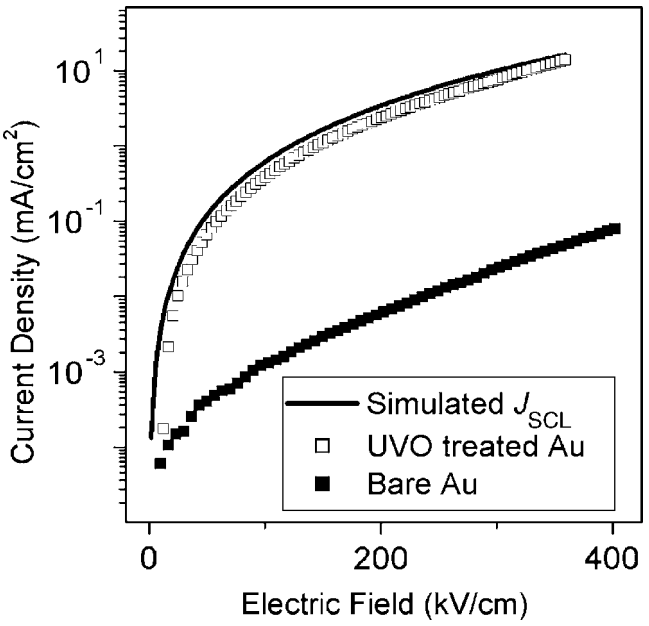

FIG. 4. Current-voltage (J-V) characteristics of Au/2TNATA/Au devices. The closed symbols represent data from the bare Au, while the open symbols are from the Au treated with UVO. The solid line is the fit to the experimental J-V curve by using the SCLC theory.

Figure 4 shows the J-V characteristic for 2TNATA, with Au as the hole-injecting anode. Ideally, if the material is trap-free and under the condition of Ohmic injection contact, the steady-state current should follow the SCLC J_{SCL}:[14]

$$J_{SCL} = \frac{9}{8}\mu_0\varepsilon_0\varepsilon_r \exp(0.89\beta\sqrt{F})\frac{F^2}{d}, \tag{1}$$

where ε_0 is the permittivity in free space, ε_r is the dielectric constant ($\sim$3 for organic materials), and d is the thickness of the organic layer. The β and μ_0 used here are derived from $\tau_{1/2}$ (Table I), i.e., 8.7×10^{-6} $(\mathrm{cm/V})^{1/2}$ and 2.9×10^{-3} $\mathrm{cm^2/V\,s}$, respectively, because the J_{SCL} describes the steady-state current density flowing through the materials. Both of the J-V curves of the samples with and without UVO treated Au are shown here. In the case of the UVO treated Au, the measured J-V curve practically overlaps with the theoretical fit using Eq. (1). So, the UVO treated Au/2TNATA contact is Ohmic and the hole conduction in 2TNATA is trap-free. However, in the case of the untreated Au, the measured J-V curve significantly deviates from the fit within the entire range of the applied electric field, showing that the injection from the bare Au into 2TNATA is non-Ohmic. The presence of an interface dipole is probably the origin of this deviation. The interface dipole originates from the spontaneous charge transfer across the metal/organic interface, which increases the energy barrier between the work function of the metal and the HOMO of the organic material.[15] The UVO treatment can increase the work function of the bare Au by introducing an ultrathin oxide layer at the Au surface.[16–18] Moreover, the ultrathin oxide layer can prevent the Au from directly contacting with 2TNATA, which minimizes the effect of the interface dipole.

Figure 5(a) shows the sequence of DI signals under different bias voltages for a sample with UVO treated Au. Each

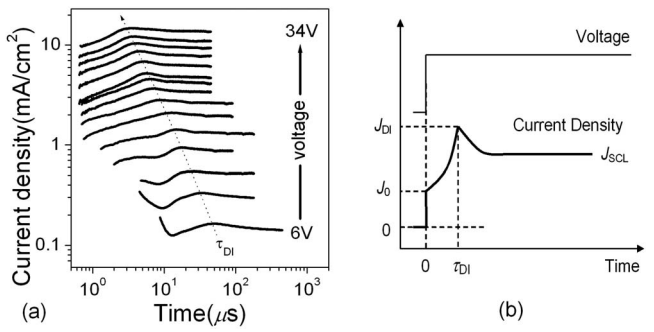

FIG. 5. (a) A sequence of DI signals of Au(treated with UVO)/2TNATA/Au under different applied voltages. The applied voltage varied in steps of 2 V starting from 6 V. (b) An ideal DI-SCLC transient.

DI transient exhibits the characteristic signature of an ideal DI-SCLC signal, as shown in Fig. 5(b). It reaches a maximum at a well-defined time τ_{DI} and decays to a steady-state value after a long time. This observation can only be found if the following conditions are satisfied: (i) the anode/organic contact is Ohmic and (ii) the organic/cathode contact is electron blocking. The transient current density $J(t)$ can be derived from Poisson's equation for a trap-free material under the condition of a unipolar Ohmic injection.[19] The carrier mobility μ_{DI} can be calculated as follows:[9,19]

$$\mu_{DI} = \frac{0.787d^2}{V\tau_{DI}}, \tag{2}$$

where τ_{DI} is the arrival time of the fastest carriers at the noninjecting electrode and is related to the space-charge-free carrier transit time τ by $\tau_{DI}=0.787\tau$; d and V are the organic layer thickness and voltage applied across the sample, respectively. The observation of the DI transients indicates that the contact between the anode and 2TNATA is Ohmic, which is consistent with the J-V experiment.

The DI transient signal progressively grows with the applied voltage, and simultaneously, τ_{DI} decreases. The mobilities of 2TNATA are extracted by Eq. (2) and compared to those independently obtained from TOF in Fig. 3. One can clearly observe that the hole mobilities extracted from the DI experiment agree well with those obtained from the TOF technique (using τ as the transit time).

Figure 6 shows the output characteristics of a 2TNATA based organic thin film transistor (OTFT) under different gate voltages and at three different temperatures. The carrier mobility can be extracted from the output characteristics of the TFT. The mobility in the saturation region is obtained from the slope of the plot of the square root of the saturated drain current I_D versus the gate voltage V_G based on[20]

$$I_D = \frac{W}{2L}\mu_{FE}C_i(V_G - V_T)^2, \tag{3}$$

where W and L are the channel width and length, respectively, C_i is the capacitance of the gate dielectric per unit area, V_T is the threshold voltage, and μ_{FE} is the field effect (FE) mobility in the saturation region. At 290 K, the FE mobility μ_{FE} and the threshold voltage V_T are 9.8×10^{-7} $\mathrm{cm^2/V\,s}$ and 25.2 V, respectively. The FE mobility is about one order of magnitude smaller than the TOF mobility

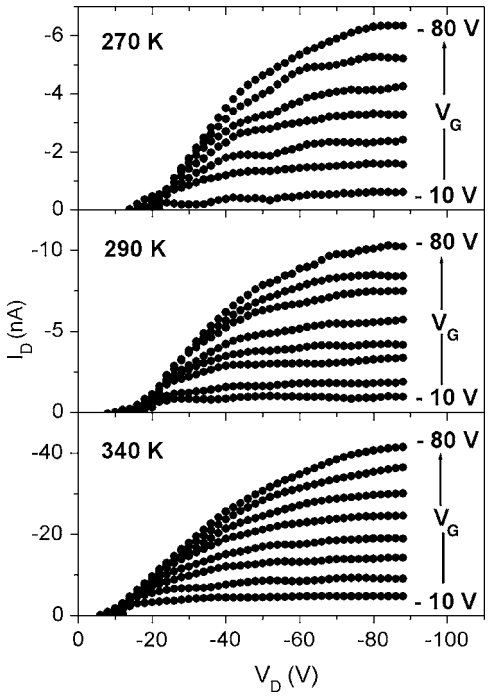

FIG. 6. Output characteristics of the bottom contact OTFT with 90 nm 2TNATA at 270, 290, and 340 K. The channel length and width are 50 μm and 9 mm, respectively.

$(1.2\times10^{-5}$ cm^2/V s). Since the FE mobility is extracted from the steady-state current, the TOF mobility derived from $\tau_{1/2}$ is considered here.

The discrepancy between the FE mobility and the TOF/DI derived mobilities is, perhaps, not surprising. In fact, similar observations were recently made for other amorphous organic materials.[21] In both the TOF and DI-SCLC experiments, free holes, once injected into 2TNATA, hop in a direction perpendicular to the organic/electrode interface. On the other hand, in the TFT experiment, injected holes tend to hop just above and parallel to the interface of the gate dielectric and 2TNATA. So, the presence of the gate dielectric layer clearly plays an important role in affecting μ_{FE}. Recently, it was proposed that there is an increase in the disorder in the organic material in the neighborhood of a polar gate dielectic.[22] The polar groups in the dielectric are randomly oriented near the active interface, resulting in an additional fluctuation of the local electrostatic field. This would broaden the density of states (DOS) of the organic material, resulting in an increase in the energetic disorder, leading to the decrease in the FE mobility.

In order to examine this concept, we performed temperature dependent measurements on the 2TNATA based OTFT. Figure 6 shows examples of the measurements. The values of the FE mobilities are then evaluated at, e.g., a field strength of 12 kV/cm (V_D=−60 V) in the saturation region) at different temperatures by using Eq. (3). The results are plotted against the inverse of the square of the temperature in Fig. 7 (circles). The extracted FE mobilities are then analyzed by the Gaussian disorder model (GDM).[23] The GDM is widely used in describing the charge transport mechanisms in many amorphous organic semiconductors.[7] In GDM, the amorphous organic material under investigation can be treated as

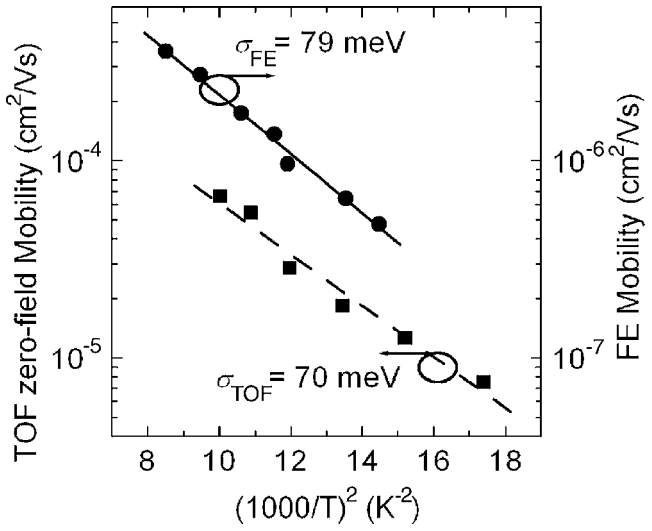

FIG. 7. Plot of the FE mobilities from TFT and zero-field mobilities (obtained from $\tau_{1/2}$) from TOF against $1/T^2$. The solid and dashed lines are the best fits to the TFT and TOF data, respectively.

an ensemble of transporting sites for hopping conduction. Each molecule is viewed as a hopping site for charge carriers. However, the sites have randomness in terms of their potential energy and spatial ordering. Within the ensemble, the hopping process is governed by the applied field F and temperature T; thus, the carrier mobility is field and temperature dependent. The GDM can be described as follows:[23]

$$\mu(F,T) = \mu_\infty \exp\left[-\left(\frac{2\sigma}{3kT}\right)^2\right] \times \exp\left\{CF^{1/2}\left[\left(\frac{\sigma}{kT}\right)^2 - \Sigma^2\right]\right\}, \quad (4)$$

where F, T, and k are the applied electric field, the absolute temperature, and the Boltzmann constant, respectively; μ_∞ is the high temperature limit of mobility; and C=2.9 $\times10^{-4}$ cm^2/V s.[23] The energetic disorder σ can be interpreted as the width of the Gaussian distribution of the DOS of energy for the transport sites; the positional disorder Σ can be considered to show the geometric randomness of the material. In order to extract the energetic disorder parameter from the TFT data, we rearrange the terms in Eq. (4) to

$$\mu(F,T) = \mu_\infty \exp\left[\left(-\frac{4}{9} + CF^{1/2}\right)\left(\frac{\sigma}{kT}\right)^2\right] \times \exp(-CF^{1/2}\Sigma^2). \quad (5)$$

From Eq. (5), we clearly see that at a fixed field strength F, $\mu(F,T)$ varies with $1/T^2$ because Σ is temperature independent. So, from a plot of $\mu(F,T)$ versus $1/T^2$, the extracted slope can be used to deduce σ. Following such a procedure, we fitted the temperature dependent μ_{FE} with Eq. (5). The solid line through the circles in Fig. 7 is the best line fit to the data, and the extracted σ was 79 meV. On the other hand, the energetic disorder can also be solely extracted from the TOF data by using the average carrier transit time $\tau_{1/2}$. In this case, we extracted the zero-field mobilities from the plot of μ_{TOF} versus $F^{1/2}$ at different temperatures. Next, the zero-

field mobilities were plotted against $1/T^2$. The experimental results are shown as solid squares in Fig. 7. The dashed line is the best fit to the TOF data. From the slope of the dashed line, we can deduce an energetic disorder parameter of 70 meV. The higher energetic disorder from the TFT concurs with the idea proposed by Veres *et al.*[22] They suggested that the polar dielectric would modify the energetic disorder of the organic material at the interface, which causes the difference between the FE and TOF mobilities. In the report, the energetic disorder of the polytriarylamines (PTAA2) was enhanced by ~30 meV with polymethylmethacrylate (PMMA) (dielectric constant ~3.8) as the gate dielectric. This difference resulted in a smaller value of the FE mobility (1.26×10^{-2} $cm^2/V\,s$), which was about two orders of magnitude smaller than that of the TOF mobility (4.86×10^{-4} $cm^2/V\,s$).

IV. CONCLUSION

TOF, DI-SCLC techniques, and TFT configuration were used to evaluate the carrier mobility of 2TNATA. The hole mobilities of 2TNATA that were obtained from DI-SCLC experiments were in good agreement with those deduced from TOF experiments. However, the FE mobilities of 2TNATA were found to be one order of magnitude smaller than the TOF mobilities. The difference did not originate from the contact effect because the organic-metal interface was demonstrated to be Ohmic by *J-V* and DI-SCLC experiments. The increase in the energetic disorder of 2TNATA in the TFT configuration under temperature dependent measurements suggest that the difference was probably due to the effect from the polar gate dielectric at the interface.

ACKNOWLEDGMENTS

Support of this research by the Research Grant Council of Hong Kong under Grant Nos. HKBU211006E and HKBU211107E is gratefully acknowledged.

[1]C. W. Tang and S. A. VanSlyke, Appl. Phys. Lett. **51**, 913 (1987).
[2]P. Peumans, A. Yakimov, and S. R. Forrest, J. Appl. Phys. **93**, 3693 (2003).
[3]G. Horowitz, J. Mater. Res. **19**, 1946 (2004).
[4]P. W. M. Blom and M. C. J. M. Vissenberg, Mater. Sci. Eng., R. **27**, 53 (2000).
[5]S. W. Liu, J. H. Lee, C. C. Lee, C. T. Chen, and J. K. Wang, Appl. Phys. Lett. **91**, 142106 (2007).
[6]S. C. Tse, K. C. Kwok, and S. K. So, Appl. Phys. Lett. **89**, 262102 (2006).
[7]S. K. So, S. C. Tse, and K. L. Tong, J. Disp. Technol. **3**, 225 (2007).
[8]P. M. Borsenberger and D. S. Weiss, *Organic Photoreceptors for Imaging Systems* (Dekker, New York, 1993), Chap. 9.
[9]S. C. Tse, S. W. Tsang, and S. K. So, J. Appl. Phys. **100**, 063708 (2006).
[10]J. Lee, K. Kim, J. H. Kim, S. Im, and D. Y. Jung, Appl. Phys. Lett. **82**, 4169 (2003).
[11]M. Kitamura, T. Imada, S. Kako, and Y. Arakawa, Jpn. J. Appl. Phys., Part 1 **43**, 2326 (2004).
[12]Y. Shirota and H. Kageyama, Chem. Rev. (Washington, D.C.) **107**, 953 (2007).
[13]S. K. So, W. K. Choi, C. H. Cheng, L. M. Leung, and C. F. Kwong, Appl. Phys. A: Mater. Sci. Process. **68**, 447 (1999).
[14]P. N. Murgatroyd, J. Phys. D **3**, 151 (1970).
[15]W. Osikowicz, M. P. de Jong, S. Braun, C. Tengstedt, M. Fahlman, and W. R. Salaneck, Appl. Phys. Lett. **88**, 193504 (2006).
[16]T. Manaka, E. Lim, R. Tamura, and M. Iwamoto, Thin Solid Films **499**, 386 (2006).
[17]D. E. King, J. Vac. Sci. Technol. A **13**, 1247 (1995).
[18]S. Rentenberger, A. Vollmer, E. Zojer, R. Schennach, and N. Kock, J. Appl. Phys. **100**, 053701 (2006).
[19]M. A. Lampert and P. Mark, *Current Injection in Solids* (Academic, New York, 1970); K. C. Kao and W. Hwang, *Electrical Transport in Solids* (Pergamon, Oxford, 1981).
[20]S. M. Sze, *Physics of Semiconductor Devices* (Wiley, New York, 1981).
[21]T. P. I. Saragi, T. F. Lieker, and J. Salbeck, Adv. Funct. Mater. **16**, 966 (2006).
[22]J. Veres, S. D. Ogier, S. W. Leeming, and D. C. Cupertino, Adv. Funct. Mater. **13**, 199 (2003).
[23]H. Bässler, Phys. Status Solidi B **175**, 15 (1993).